

Removal of perchlorate from wastewater through adsorption and reductive degradation using Ni-Fe bimetallic nanoparticles supported on modified activated carbon: A simple strategy to degrade persistent pollutants

Ali Reza Zarei[✉], Ali Moloudi

Faculty of Chemistry and Chemical Engineering, Malek Ashtar University of Technology, Tehran, Iran

Date of submission: 04 May 2019, **Date of acceptance:** 02 Nov 2019

ABSTRACT

In the present study, nickel and iron (Ni/Fe) bimetallic nanoparticles (Ni-Fe NPs) were produced in the presence of activated carbon (AC) to prepare supported Ni/Fe bimetallic nanoparticles (Ni-Fe NPs/AC). The NPs were modified using cetylpyridinium chloride and used for the simultaneous adsorption and degradation of perchlorate. Synthesized Ni-Fe NPs/AC was characterized using FE-SEM, EDS, and XRD. The influential factors in the removal of perchlorate by Ni-Fe NPs/AC were optimized based on experimental design. According to the results, adsorption and degradation efficiencies were 96.98% and 78.81%, respectively, which could be achieved to the efficiency of nearly 100% by increasing the process time to 110 minutes. Reaction kinetics complied with the pseudo-first-order characteristics. Moreover, the rate constant of adsorption and degradation were estimated at 0.0848 and 0.0199 min⁻¹ at 303 K, and the activation energy for adsorption and degradation was 42.39 and 12.47 kJ/mol, respectively. The proposed method could effectively remove perchlorate from well water and industrial wastewater. Therefore, Ni-Fe NPs/AC could be an effective nanomaterial for the complete degradation of perchlorate. This novel method could also remove persistent organic and inorganic pollutants and promote the industrial application of bimetallic NPs in environmental remediation.

Keywords: Perchlorate, Adsorption, Reductive degradation, Activated carbon, Ni/Fe bimetallic nanoparticles

Introduction

Perchlorate (ClO₄⁻) is a persistent inorganic pollutant, which is normally produced during the manufacturing, storage, and assessment of solid rocket motors, with ammonium perchlorate (AP) used as an oxidizer.¹⁻³ The recovery of propellant from solid rocket motors is considered to be an important source of perchlorate pollution, leading to the generation of wastewater in the form of AP.⁴ Perchlorate competes with iodide for uptake into the thyroid gland by the sodium-iodide symporter (NIS) since iodide resembles perchlorate in terms of the ionic charge and size, as well as the conveyance mechanism in the membrane of

thyroid cells.⁵ This may interrupt the production of thyroid hormones, thereby disturbing human metabolism.⁶⁻⁸

In order to determine the effects of perchlorate on human health, an extensive database of animal toxicity studies has been developed in accordance with the related risk assessment guidelines and perchlorate mechanism. According to the United States National Academy of Sciences (US NAS), 0.0007 milligram of perchlorate/kg/day is an oral reference dose (RfD), with the drinking water equivalent dose of 24.5 µg/l. Moreover, the US EPA has issued an Interim Drinking Water Health Advisory for exposure to perchlorate at the concentration of 15 µg/l in water.⁹ Therefore, special attention must be paid to the removal of perchlorate from water and wastewater.

Recently, various treatment technologies have been applied for the removal of perchlorate from water, including biological removal,^{9,10} ion

✉ Ali Reza Zarei
zareei1349@gmail.com

Citation: Zarei AR, Moloudi A. Removal of perchlorate from wastewater through adsorption and reductive degradation using Ni-Fe bimetallic nanoparticles supported on modified activated carbon: A simple strategy to degrade persistent pollutants. J Adv Environ Health Res 2019; 7(4): 213-224

exchange (IX),¹¹ activated carbon adsorption,¹² filtration,¹³ and chemical reduction.¹⁴⁻¹⁶ Among these methods, chemical reduction techniques have been more widely considered for the destruction of perchlorate to nontoxic chloride ion. Due to their extremely small particle size and large reactive surface area, iron-based nanoparticles have attracted attention for the remediation of groundwater contaminants.^{17,18} In fact, metal nanoparticles without stabilizer are agglomerated on the micron scale, and several methods have been developed to modify their reactivity and enhance their surface area.¹⁷ In a study in this regard, He *et al.* used carboxy methyl cellulose (CMC) as a stabilizer for the preparation of nanozerovalent iron (nZVI).^{19,20} Furthermore, Xiong *et al.* have reported that the degradation rate of perchlorate by nZVI stabilized with starch and CMC is faster compared to nZVI.²¹ Other findings have also denoted that the reduction rate of bromate and nitrate using nZVI modified in aqueous ethanol solution is faster compared to nZVI.^{22,23} According to the results obtained by Xiong *et al.*, since the surface of ZVI nanoparticles is oxidized to iron oxides (Fe₂O₃), it could rapidly adsorb perchlorate from water.²¹ On the other hand, Choi *et al.* investigated the dechlorination of polychlorinated biphenyls, suggesting an effective strategy by applying a series of granular activated carbon (GAC) composites containing iron/palladium (Fe/Pd) bimetallic nanoparticles.²⁴ A similar paradigm was also reported by Zhu *et al.*, in which nZVI was used along with GAC for the removal of arsenic.²⁵

The present study aimed to improve the degradation efficiency of perchlorate as a persistent inorganic pollutant to nontoxic chloride ion via simultaneous adsorption and reductive degradation using Ni-Fe NPs/AC. Initially, Ni/Fe bimetallic nanoparticles were synthesized in the presence of activated carbon (AC) in order to prepare the supported nanoparticles (Ni-Fe NPs/AC). Afterwards, the nanoparticles were used for the degradation of perchlorate from water and wastewater after modification with cetylpyridinium chloride (CPC).

Materials and Methods

Apparatus

A UV-Vis spectrophotometer (model: Hitachi 3310) was applied for the photometric determination of perchlorate and iron ion in the aqueous solutions, and pH was measured using a pH meter (PH.Z.S.PTR79). In addition, analysis of the synthesized NPs was performed using an X-Pert Philips XRD instrument and an electron microscopy (model: Sigma, Zeiss Ltd. Co., Germany).

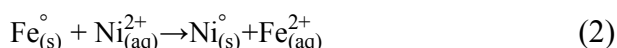
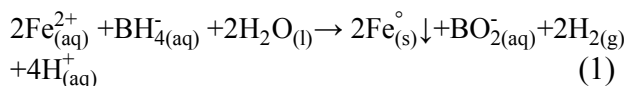
Materials

Deionized (DI) water was utilized to prepare the solutions in the experiments, and all the applied reagents were of the analytical grade. Starch ([C₁₂H₂₂O₁₁]_n>99%), ferrous chloride (FeCl₂·6H₂O>99%), potassium perchlorate (KClO₄>99%), CPC, acetic acid (CH₃COOH), methylene blue, sulfuric acid (H₂SO₄), sodium acetate (CH₃COONa), and chloroform (CHCl₃) were purchased from Merck company (Merck, Darmstadt, Germany). In addition, sodium borohydride (NaBH₄, 98%) was obtained from Fluka Company. Nickel (II) acetate tetrahydrate (Ni (CH₃COO)₂·4H₂O), 1,10-phenanthroline (C₁₂H₈N₂), and hydroxylamine (NH₂OH) were purchased from Sigma-Aldrich (USA).

Synthesis of Ni-Fe NPs/AC

The synthesis of Ni-Fe NPs/AC was performed in four steps. Initially, the AC was washed by soaking in 1M HNO₃ for 24 hours, followed by washing with DI water repeatedly to completely remove the acid. Afterwards, 2.0 gram of the treated AC was mixed with 100 milliliters of DI water, and the solution was heated to the boiling temperature for five minutes. After the isolation of AC via centrifugation, it was dried overnight at the temperature of 120 °C. In the second step, 3.3 grams of FeCl₂·6H₂O and 1.24 grams of Ni(CH₃COO)₂·4 H₂O were mixed with one gram of AC, which had been prepared in the previous stage in 50 milliliters of DI water, and the mixture was exposed to nitrogen gas for deoxygenation for 30 minutes. In the third step, the NaBH₄ solution (3.15 g in 50 ml of DI water)

was added to the solution under the nitrogen gas slowly in order to reduce Fe(II) and Ni(II) to the nickel-iron bimetallic nanoparticles using Eqs. 1-2 and the mixture was stirred for approximately two hours until no significant H₂ production was observed.



In the fourth step, the surface of Ni-Fe NPs/AC, which had been prepared in the previous stage, was modified using a surfactant. To do so, the surface was washed with DI water three times, added to 0.5% (w/v) CPC solution, and stirred for three hours using a mechanical stirrer. The modified Ni-Fe NPs/AC was isolated using a magnet, washed with DI water, and placed at the temperature of 70 °C for three hours in a vacuum oven. Fig. 1 depicts the entire scheme of the synthesis procedure.

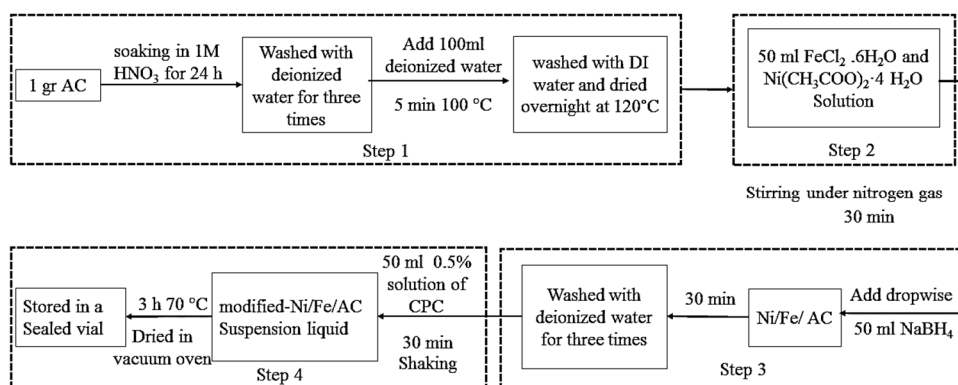


Fig. 1. Schematic illustration of the preparation of Ni/Fe nanoparticles on AC (The whole procedure was bubbled with N₂ gas)

Removal of perchlorate from the aqueous solutions

In optimal conditions, 50 milliliters of the perchlorate solution ($C_0=20 \mu\text{g/ml}$) was initially purged under N₂ gas for 10 minutes in a three-necked flask, and the pH of the solution was adjusted at 5.6. Following that, 100 milligrams of the modified Ni-Fe NPs/AC was added, and the solution was stirred at the temperature of 35 °C for 90 minutes. Finally, the Ni-Fe NPs/AC was collected using a magnet (1.2 Tesla), and the concentration of perchlorate (C_t) in the stripped solution was determined spectrophotometrically using Eq. 3. Moreover, the removal efficiency was evaluated using the same equation, as follows:

$$\%RE = \frac{C_0 - C}{C_0} \times 100 \quad (3)$$

where RE is the removal efficiency (%) of perchlorate, and C_0 and C represent perchlorate concentration at the initial and appropriate

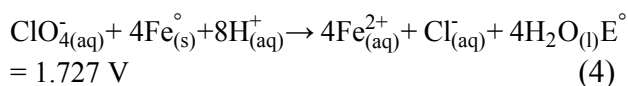
times of the process, respectively. In addition, the produced Fe²⁺ ion was determined as described in the following section in order to determine the reductive degradation efficiency.

Perchlorate determination for evaluation of adsorption efficiency

Perchlorate adsorption efficiency was assessed using a spectrophotometric method based on the ion pairing of perchlorate with methylene blue in acidic media and extraction of perchlorate into the chloroform solvent.²⁶ Moreover, an aliquot of the perchlorate solution (range: 1.0-10 $\mu\text{g/ml}$), sulfuric acid solution (1.0 ml of 2 mol/l), and methylene blue solution (1.0 ml of 1.5×10^{-3} mol/l) were transferred into a 10-milliliter test tube and stirred for 5 minutes. Following that, three milliliters of chloroform was transferred to the test tube and shaken for five minutes, and the absorbance of the organic phase was measured at 676 nanometers.

Evaluation of reductive degradation efficiency

In the degradation process of perchlorate by nanoparticles, the Fe^{2+} ion was produced through the Eq. 4:



As a result, the degradation efficiency of perchlorate could be evaluated using the produced Fe^{2+} ion. To this end, the concentration of the Fe^{2+} ion in the solution was defined based on the complex reaction of Fe^{2+} with 1,10-phenanthroline (O-Ph) to form a colored product.²⁷ In this process, an aliquot of the Fe(II) solution (1.0-20 $\mu\text{g}/\text{ml}$) was added to a 10-milliliter volumetric flask with 0.5 milliliter of hydroxylamine hydrochloride (10% [w/v]). The solution was shaken for 10 minutes for the conversion of Fe(III) into Fe(II).

At the next stage, 0.5 milliliter of 0.3% (w/v) 1,10-phenanthroline solution was added to the volumetric flask and shaken for 10 minutes. Afterwards, the volumetric flask was diluted with DI water to the mark, and the absorbance was measured at 510 nanometers. In addition, a blank solution containing only 63 milligrams of modified Ni-Fe NPs/AC was imposed based on the same procedure in order to determine the level of the produced Fe^{2+} ion due to possible oxidation by dissolved oxygen in the solution.

Optimization based on experimental design

Response surface methodology (RSM) is a common mathematical and statistical method for the optimization of experimental variables, which examines the effects of an independent variable alone or in combination.²⁸ Furthermore, this methodology generates a mathematical model to analyze the effects of the independent variables that accurately describe the overall process.²⁹

In the design of the experiments in this study, the most important step was the selection of the influential factors in the desired response. As such, several factors had to be removed due to their negligible impact. In the current

research, the effects of nanoparticle dosage, temperature, initial pH, and time on removal efficiency were estimated using RSM. In addition, a central composite design (CCD) with three factors was used, and an additional 20 media optimization experiments were designed in the CCD.

Data analysis was performed in the Design Expert software version 7.1.5, and the generation of the response surface graphics was achieved as well. Moreover, the analysis of variance (ANOVA) was applied, and the polynomial model equation quality was statistically determined using the coefficient of determination (R^2), with its statistical significance obtained by the F-test.

Results and Discussion

Characterization of the AC-supported Fe-Ni nanoparticles

The prepared Ni-Fe NPs/AC was evaluated using scanning electron microscopy (SEM)-energy dispersive X-ray (EDX) with the magnification of 60,000, along with the EDX mappings of iron and nickel (Figures 2- 3). The nanoparticle size was calculated within the range of 20-70 nanometers. As was observed in the EDX mapping, iron and nickel were located near each other on the AC. Furthermore, an oxygen peak was detected due to oxidation during sample preparation. Nevertheless, the atomic ratio of iron to nickel was estimated at 3:100.

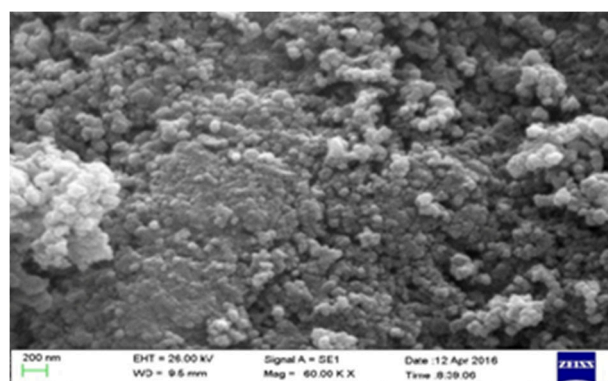


Fig. 2. Image of laboratory-synthesized Ni/Fe nanoparticles on AC obtained with a field-emission scanning electron microscope (SEM) (60.00 Kx). Eighty percent particles had diameters less than 100 nm

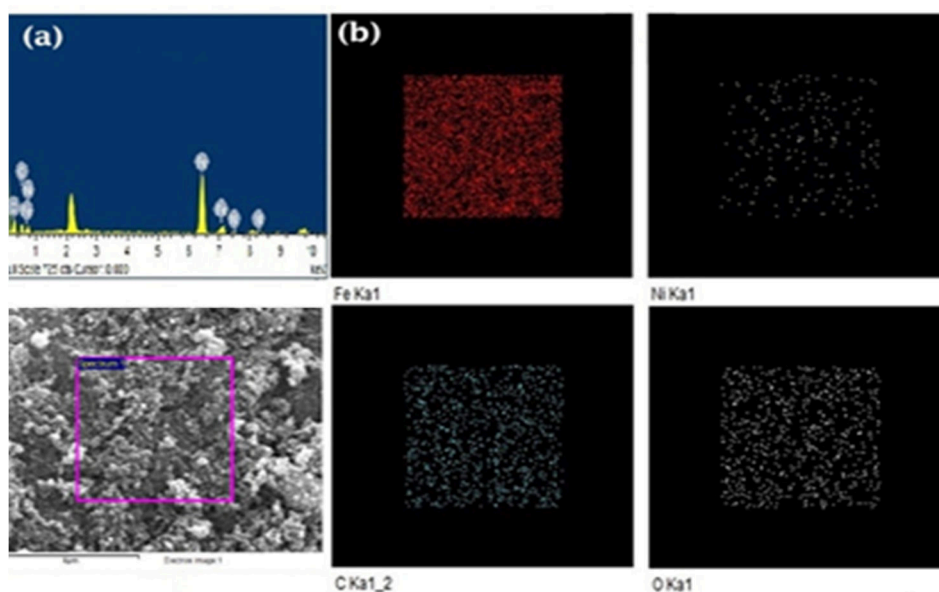


Fig. 3. (a) EDS spectrum of Ni/Fe nanoparticles on AC (vacuum, 5×10^{-7} torr; lens current, 1.8 A; voltage, 20 kV), (b) EDS elemental mapping of the Ni/Fe nanoparticles on AC

Fig. 4 shows the X-ray diffraction (XRD) results for fresh Ni-Fe NPs/AC. The characteristic peaks of iron appear at 44.64° (main peak), and the peaks assigned at 65.16° and 80.16° belonged to nickel.

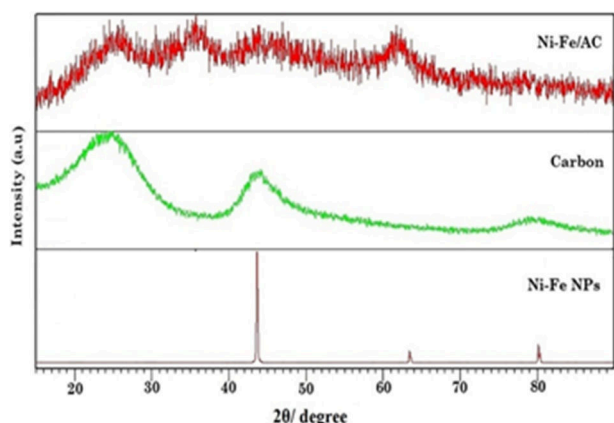


Fig. 4. XRD spectra of nanoscale Ni/Fe particles on AC

Experimental design

We assessed three influential factors in the removal process, including the initial pH, temperature, and time. Table 1 shows the range of the influential factors and their levels. Due to the adsorption process and subsequent reductive

degradation of perchlorate by Ni-Fe NPs/AC, the adsorption and absorption efficiency were modeled separately. To this end, 20 tests with various operational conditions were developed based on the CCD methodology (Table 2). The tests were performed, and the regression analysis of the adsorption efficiency indicated that the data could be modeled by a second-order polynomial equation, as Eq. 5:

$$\text{Adsorption efficiency (\%)} = +90.82 - 13.97A - 14.87B + 0.89C + 1.12AB - 1.63AC - 6.7A^2 - 10.11B^2 + 0.74C^2 + 9.49A^2B + 7.98A^2C + 7.85AB^2 \quad (5)$$

ANOVA was performed for the response quadratic model, and the P-value of less than 0.05 indicated that the model terms were significant, while the values higher than 0.10 were not considered significant (Table 3). According to the results of the present study, the most significant model terms included pH, temperature (T), time, $\text{pH} \times T$, $\text{pH} \times \text{time}$, pH^2 , T^2 , time^2 , $\text{pH}^2 \times T$, $\text{pH}^2 \times \text{time}$, and $\text{pH} \times T^2$, which were maintained.

Table 1. The range and levels of the independent variables

Factor	Parameter	Units	Type	Low Actual	High Actual	Low Coded	High Coded	Mean	Std. Dev.
A	pH		Numeric	5	8	-1	1	6.5	1.24
B	T	$^\circ\text{C}$	Numeric	30	60	-1	1	45	12.39
C	time	min	Numeric	50	100	-1	1	75	20.65

Table 2. The designed experiments by CCD for the removal process

Run	pH	Temperature (°C)	Time (min)	Adsorption efficiency (%)	Reductive degradation efficiency (%)
1	5.00	30.00	50.00	76.00	64.00
2	8.00	30.00	50.00	64.00	6.00
3	5.00	60.00	50.00	62.00	45.00
4	8.00	60.00	50.00	56.00	12.00
5	5.00	30.00	100.00	96.00	76.00
6	8.00	30.00	100.00	79.00	67.00
7	5.00	60.00	100.00	84.00	36.00
8	8.00	60.00	100.00	70.00	10.00
9	3.98	45.00	75.00	95.00	60.00
10	9.02	45.00	75.00	48.00	15.00
11	6.50	19.77	75.00	87.00	57.00
12	6.50	70.23	75.00	37.00	11.00
13	6.50	45.00	32.96	87.00	40.00
14	6.50	45.00	117.04	90.00	50.00
15	6.50	45.00	75.00	93.00	69.00
16	6.50	45.00	75.00	89.00	65.00
17	6.50	45.00	75.00	90.00	70.00
18	6.50	45.00	75.00	90.00	69.00
19	6.50	45.00	75.00	91.00	65.00
20	6.50	45.00	75.00	92.00	68.00

According to the information in Table 3, higher temperature reduced the surface adsorption of Ni-Fe NPs/AC, followed by the adsorption efficiency of the perchlorate. On the

other hand, increased time provided adequate time to adsorb perchlorate onto the AC surface, thereby increasing the adsorption efficiency of perchlorate.

Table 3. Analysis of variance for the response surface reduced cubic mode

Response1: Adsorption efficiency (%)						
Source	Sum of squares	df	Mean square	F-Value	p-value	Prob> F
Model	5514.62	11	501.33	318.70	< 0.0001	Significant
A-pH	1104.50	1	1104.50	702.14	< 0.0001	
B-T	1250.00	1	1250.00	794.63	< 0.0001	
C-time	4.50	1	4.50	2.86	0.1292	
AB	10.13	1	10.13	6.44	0.0349	
AC	21.13	1	21.13	13.43	0.0064	
A ²	656.96	1	656.96	417.63	< 0.0001	
B ²	1473.16	1	1473.16	936.5	< 0.0001	
C ²	7.92	1	7.92	5.04	0.0551	
A ² B	298.44	1	298.44	189.72	< 0.0001	
A ² C	211.18	1	211.18	134.25	< 0.0001	
AB ²	204.10	1	204.10	129.75	< 0.0001	
Residual	12.58	8	1.57			
Lack of Fit	1.75	3	0.58	0.27	0.8453	Not significant
Pure Error	10.83	5	2.17			
Cor Total	5527.20	19				

Predicted R-squared represents the capability of the model for the prediction of the response value. In the present study, predicted R-squared was consistent with the adjusted R-squared. On the same note, adequate precision is

used to measure the signal to the noise ratio, and ratios higher than four are considered desirable; the ratio was estimated at 60.852 in the present study, indicating an adequate signal. In addition, R² explains the overall performance of the

model, and adjusted R² demonstrated the degree of correlation between the observed and predicted values.³⁰ For the model in the current research, R² and adjusted R² were calculated to be 0.9977 and 0.9946, respectively, which indicated that the selected model could be used to predict the process behavior in the design space. According to the results of the performed tests and regression analysis for the reductive degradation of perchlorate by Ni-Fe NPs/AC, the data could be modeled by a second-order polynomial equation, as Eq. 6:

$$\text{Reductive degradation efficiency (\%)} = + 67.59 - 14.77A - 13.72B + 2.97C + 7.00AC - 10.50B C - 0.16A^2 - 1.39B^2 - 7.50 C^2 - 5.25AB C + 4.78A^2 C \quad (6)$$

The significant model terms that were maintained in the present study included pH, T, time, pH², T², and time², and the interactions of pH, and time with T, pH², and time were also considered significant. On the other hand, the

findings demonstrated that perchlorate degradation is favored at acidic pH since iron acts as an electron producer to reduce activity with the production of iron hydroxide at higher pH, while iron hydroxide covers the Fe⁰ surface in order to impede further reduction.^{31,32}

Table 4 shows the results of ANOVA for the reduced quadratic model. The F-value of the modified model (145.35) implied that the model was significant. In addition, the F-test with a low P-value (>0.0001) specified that the model was significant. The validity of the model could be assessed by determining the R² coefficient, which was calculated to be 0.9938, indicating that more than 95% of the variability in the response could be explained by the model. The predicted coefficient (predicted R²= 0.9260) was also consistent with the adjusted coefficient (adjusted R²= 0.9870), and these values displayed a high degree of correlation between the predicted and experimental values.

Table 4. Analysis of variance for the response surface reduced cubic mode

Source	Sum of Squares	df	Mean Square	F Value	p-value Prob> F	
Model	11083.13	10	1108.31	145.35	< 0.0001	Significant
A-pH	2978.36	1	2978.36	390.61	< 0.0001	
B-T	2570.48	1	2570.48	337.12	< 0.0001	
C-time	50.00	1	50.00	6.56	0.0306	
AC	392.00	1	392.00	51.41	< 0.0001	
BC	882.00	1	882.00	115.67	< 0.0001	
A ²	1486.37	1	1486.37	194.94	< 0.0001	
B ²	1870.66	1	1870.66	245.34	< 0.0001	
C ²	811.52	1	811.52	106.43	< 0.0001	
ABC	220.50	1	220.50	28.92	0.0004	
A ² C	75.62	1	75.62	9.92	0.0118	
Residual	68.62	9	7.62			
Lack of Fit	45.29	4	11.32	2.43	0.1786	Not significant
Pure Error	23.33	5	4.67			
Cor Total	11151.75	19				

In the present study, three dimensional response surface curves (3D) were plotted to explain the interactions of the medium components, and each plot showed the effects of two factors, while the other factors were maintained at the zero level. These response surface plots were obtained through the visual interpretation of the interactions between the two variables. The presence of impeccable

interaction between these independent variables demonstrated the saddle/elliptical nature of the contour plots.^{33,34}

Fig. 5 depicts the 3D response surface graph for the sorption of perchlorate. Moreover, Figures 5a and 5b show the interactions between pH-T and pH-time, respectively. According to the obtained results, the maximum response occurred at the lowest pH and T, while the

highest levels were observed at the reaction time. The 3D graph in Figures 5c and 5d illustrates the reductive interaction between pH-time and T-time. At the optimum level, the

maximum response occurred at the lowest levels of T and pH, while the highest levels were detected at the reaction time.

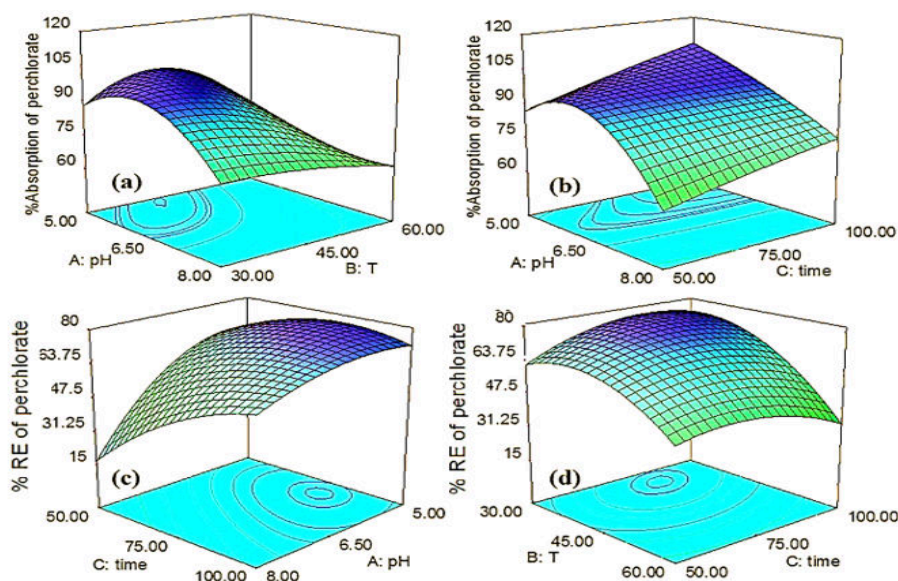


Fig. 5. Response surface graph of the variation of the adsorption efficiency, (a) function of the initial pH and temperature (time = 86.56 min), (b) function of time and pH ($T=33.94\text{ }^{\circ}\text{C}$). (c) function of the initial pH and time ($T=33.94\text{ }^{\circ}\text{C}$), (d) function of time and temperature ($\text{pH}=5.94$)

Optimization of the operating parameters

In the current research, optimization was performed by maintaining all the responses within the desired ranges using RSM, and all the variables were maintained within the range. According to the obtained results at the optimal conditions ($\text{pH}: 5.94$, $\text{time}=86.56\text{ min}$, $T=33.94\text{ }^{\circ}\text{C}$), the adsorption efficiency of perchlorate was estimated at 99.35%, and the degradation efficiency was determined to be 78.38%. In addition, the degradation efficiency could be improved up to 100% by increasing the time of the process to 110 minutes.

Kinetic studies

The removal of soluble perchlorate was performed through a multistep process, and pseudo-first-order kinetics (Eq. 7) was used for the treatment of perchlorate removal rate.

$$\ln\left(\frac{C}{C_0}\right) = -k_{\text{obs}} \cdot t \quad (7)$$

In Eq. 7, k_{obs} is the measured rate constant (1/min), C_0 and C represent the perchlorate concentration ($\mu\text{g}/\text{ml}$) before and after removal, respectively, and t shows time (min). Fig. 6 depicts $\log(C/C_0)$ as a function of the removal time, while k_{obs} is the slope of this line with the correlated parameters observed to have high correlation coefficients ($R^2 > 0.98$). However, the obtained results indicated that the removal process was divided into two parts; the first part appeared within the first 50 minutes due to the combination of adsorption on AC and perchlorate reduction reaction with the Ni/Fe nanoalloys (Fig. 6 a). According to the findings of the current research, adsorption onto the AC attracted perchlorate to accumulate around the Ni/Fe nanoalloys, thereby resulting in the rapid reduction rate. Furthermore, a relatively gradual reduction occurred in the second step, and the reaction rate was affected by intra-particle diffusion and decreased AC surface area (Fig. 6 b). Fig. 6 shows the good fitness of the experimental data for the adsorption and

reduction steps using the first-order kinetic model with the rate constant of 0.0848 and 0.0199 min⁻¹, respectively. On the other hand, the Ni/Fe nanoalloys were observed to play a key role in the function of electrons for the

reduction of the perchlorate ions, which in turn caused the reaction to remain rapid. Evidently, the decreased Ni/Fe nanoalloys and filling of the pores on the surface of the AC led to the gradual reduction of the reaction rate.

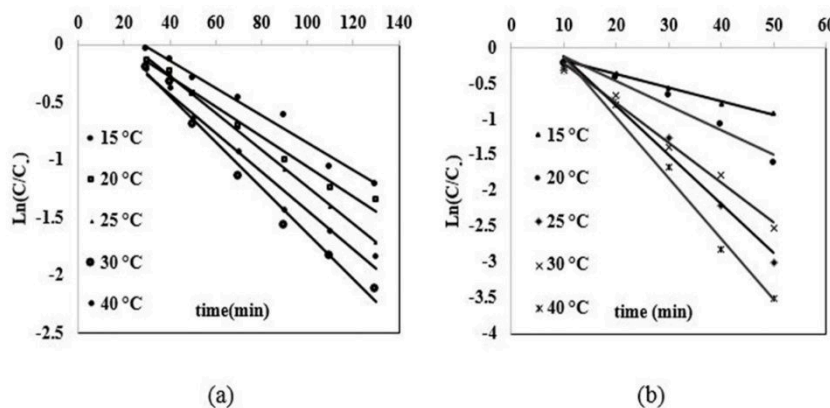


Fig. 6. Fitting first-order model to the experimental perchlorate removal rate (a) adsorption step, (b) reduction step

Fig. 7 shows the Arrhenius plot (Eq. 8) and log (k) versus 1/T for the reaction of the nanoparticles.

$$\ln k = \ln A - E_a/RT \quad (8)$$

where A is the pre-exponential factor, k shows the constant rate, T is the temperature (K), E_a represents the activation energy, and R is the

ideal gas constant. The average E_a value for the adsorption and degradation processes was calculated to be 42.39 and 12.47 kJ/mol, respectively. As a result, the degradation rate using the Ni-Fe NPs/AC was more efficient compared to the use of nanoparticles, so that they could be used for perchlorate degradation (Table 5).

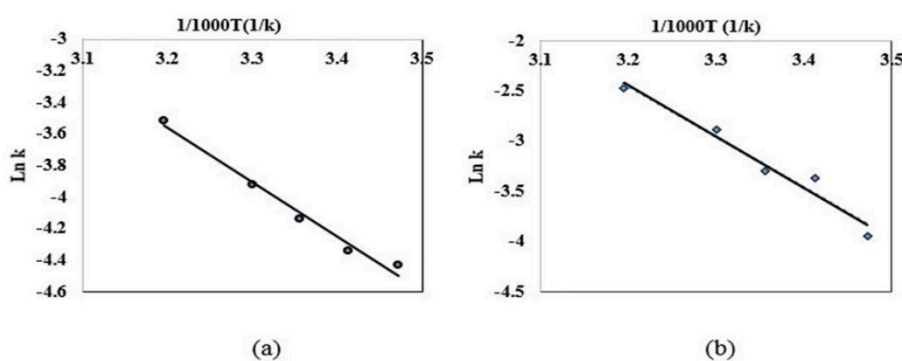


Fig. 7. Arrhenius plots of the natural logarithm of rate constant (k) vs. 1/T (a) adsorption step, and (b) reductive degradation step

Table 5. Comparison of efficiency the proposed method with other reported methods in reductive degradation of perchlorate from aqueous solutions

Nanoparticles	Time	Temperature (°C)	%RE	K (min ⁻¹)	E _a (kJ mol ⁻¹)	Reference
nZVI	36 h	75	95	0.0253	79.02	15
CMC-nZVI	6 h	110	90	0.0164	52.59	20
Fe/GAC	12 h	25	86	0.0025	9.65	7
Ni-Fe NPs/AC	110 min	34	100	0.0199	12.47	This work

Adsorption isotherm studies

The study of the adsorption isotherms yielded the data on the adsorption capacity and surface properties, providing a better understanding regarding the improvement of the adsorption system and obtaining the affinity of the adsorbent. The Freundlich and Langmuir equilibrium model isotherms were also analyzed, and the number of adsorbed milligrams per gram of the adsorbent (q_e) versus the residual concentration (C_e) showed the equilibrium adsorption isotherm model. In order to determine the equilibrium isotherm, the adsorption tests were carried out by adding 100 milliliters of the perchlorate solution (10-50 $\mu\text{g/ml}$) and 100 milligrams of the Ni-Fe NPs/AC to a three-necked flask. The solution was preserved at the pH of 5.6, shaken at 250 rpm using a mechanical stirrer at the temperature of 34 $^\circ\text{C}$, and maintained for 110 minutes in order to reach the adsorption equilibrium. At the end of each experiment and after the separation of perchlorate from the sorbent, the residual perchlorate concentration was measured using the spectrophotometric method. Moreover, q_e (mg/g) was calculated using Eq. 9:

$$q_e = \frac{V(C_0 - C_e)}{m} \quad (9)$$

where V is the volume of the experimental solution (l), C_0 shows the initial concentration of perchlorate (mg/l), and m represents the dry

weight of Ni-Fe NPs/AC (g). The linearized Langmuir isotherm could be expressed, as Eq. 10:

$$q_e = \frac{q_{\max} \cdot K_L \cdot C_e}{1 + K_L \cdot C_e} \quad (10)$$

where K_L and q_{\max} are the adsorption energy (l/mg) and Langmuir constants related to the adsorption capacity (maximum amount adsorbed per gram of the adsorbent [mg/g]), respectively. The slope and intercept of the linear plot of C_e/q_e against C_e show the values of q_{\max} and K_L , respectively. Table 6 shows the parameters of the Langmuir equation.

The linearized form of the Freundlich adsorption isotherm equation is as Eq. 11:

$$\ln q_e = \ln K_f + \left(\frac{1}{n}\right) \ln C_e \quad (11)$$

where q_e is the amount adsorbed at the equilibrium (mg/g), C_e is the equilibrium concentration (mg/l), K_f ($\text{mg}^{1-1/n} \text{l}^{1/n} / \text{g}$) denotes the Freundlich constants depending on the temperature and given adsorbent-adsorbate couple, n is an empirical parameter of sorption, and K_f indicates the adsorption capacity. These values were calculated based on the intercept and slope of the plots $\ln q_e$ versus $\ln C_e$ (Table 6). Furthermore, the Langmuir isotherm model indicated the homogeneous distribution of the active sites on the surface of Ni-Fe NPs/AC, thereby better explaining the adsorption process of perchlorate onto the AC ($R^2 > 0.996$).

Table 6. Parameters of adsorption isotherm models for the adsorption of perchlorate on Ni-Fe NPs/AC adsorbent

Langmuir				Freundlich		
aL(L/mg)	K_L (L/g)	$q_{\max}=[K_L/a_L]$ (mg/g)	R^2	K_F ($\text{mg}^{1-1/n} \text{L}^{1/n} / \text{g}$)	1/n	R^2
0.312	6.37	20.41	0.996	5.42	0.46	0.945

Application of the proposed method

The proposed method in the present study was applied for the removal of perchlorate from well water and industrial wastewater. In brief, 50 milliliters of perchlorate solution (20 $\mu\text{g/mL}$) was prepared using well water to investigate the effects of the matrix and interfering species. After the removal of perchlorate in optimal conditions, the adsorption and degradation efficiencies were estimated at 98% and 90%,

respectively. Moreover, the removal of perchlorate was carried out in a wastewater sample obtained from a perchlorate production factory (with a concentration of 300 $\mu\text{g/mL}$). For this objective, 5 mL of wastewater was transferred into a 50-milliliter volumetric flask and was diluted to the mark with distilled water, and degraded using the proposed in optimum conditions, and the adsorption and degradation efficiencies were estimated at 96% and 89%,

respectively. Therefore, it could be concluded that the method could effectively remove perchlorate from wastewater samples, and the sample matrix has no effect on the removal efficiency of perchlorate from aqueous solutions.

Conclusion

Since perchlorate is a persistent inorganic pollutant, its degradation to chloride ion as a nontoxic compound at low temperatures is an issue requiring adequate research. We aimed to develop an efficient method to degrade perchlorate through a reductive reaction in an aqueous environment. As such, we synthesized Ni/Fe nanoparticles in the presence of activated carbon based on a reductive reaction with sodium borohydride. As a result, the formed nanoparticles were protected by activated carbon. Following that, the surface of activate carbon was modified using cetylpyridinium chloride as the cationic surfactant, so that the absorption of perchlorate would be facilitated. Simultaneous with the adsorption of perchlorate, its degradation was quickly accomplished using the Ni/Fe bimetallic nanoparticles. Therefore, it is concluded that the proposed technique is a promising strategy to improve the degradation efficiency of persistent organic and inorganic pollutants using nanoparticles.

References

1. Urbansky ET. Perchlorate chemistry: implications for analysis and remediation. *Bioremediat J* 1998; 2(2): 81-95.
2. Urbansky ET, Schock M. Issues in managing the risks associated with perchlorate in drinking water. *J Environ Manag* 1999; 56(2): 79-95.
3. Liu Y, Cheng Y, Lv S, Liu C, Lai J, Luo G. Synthesis of nano-CuI and its catalytic activity in the thermal decomposition of ammonium perchlorate. *Res Chem Intermed* 2015; 41(6): 3885-392.
4. Magnuson ML, Urbansky ET, Kelty CA. Determination of perchlorate at trace levels in drinking water by ion-pair extraction with electrospray ionization mass spectrometry. *Anal Chem* 2000; 72(1): 25-29.
5. Tan K, Anderson TA, Jackson WA. Degradation kinetics of perchlorate in sediments and soils. *Water Air Soil Pollut* 2004; 151(1): 245-59.
6. Urbansky ET. Perchlorate as an environmental contaminant. *Environ Sci Pollut Res* 2002; 9(3): 187-92.
7. Xu J, Gao N, Tang Y, Deng Y, Sui M. Perchlorate removal using granular activated carbon supported iron compounds: Synthesis, characterization and reactivity. *J Environ Sci* 2010; 22(11): 1807-13.
8. Wolff J. Perchlorate and the thyroid gland. *Pharmacol Rev* 1998; 50(1): 89-106.
9. Logan BE, LaPoint D. Treatment of perchlorate- and nitrate-contaminated groundwater in an autotrophic, gas phase, packed-bed bioreactor. *Water Res* 2002; 36(14): 3647-53.
10. McCarty PL, Meyer TE. Numerical model for biological fluidized-bed reactor treatment of perchlorate-contaminated groundwater. *Environ Sci Technol* 2005; 39(3): 850-8.
11. Xiong Z, Dimick P, Zhao D, Kney A, Tavakoli J. Removal of perchlorate from contaminated water using a regenerable polymeric ligand exchanger. *Sep Sci Technol* 2006; 41(11): 2555-74.
12. Chen W, Cannon FS, Rangel-Mendez JR. Ammonia-tailoring of GAC to enhance perchlorate removal. II: Perchlorate adsorption. *Carbon* 2005; 43(3): 581-90.
13. Yoon J, Yoon Y, Amy G, Cho J, Foss D, Kim TH. Use of surfactant modified ultrafiltration for perchlorate (ClO_4^-) removal. *Water Res* 2001; 37(9): 2001-201.
14. Moore AM, De Leon CH, Young TM. Rate and extent of aqueous perchlorate removal by iron surfaces. *Environ Sci Technol* 2003; 37(14): 3189-98.
15. Cao J, Elliott D, Zhang W. Perchlorate reduction by nanoscale iron particles. *J Nanopart Res* 2005; 7(4-5): 499-506.
16. Lien HL, Yu CC, Lee YC. Perchlorate removal by acidified zero-valent aluminum and aluminum hydroxide. *Chemosphere* 2010; 80(8):888-93.
17. Saffari M, Karimian N, Ronaghi A, Yasrebi J, Ghasemi- Faseai R. Reduction of chromium toxicity by applying various soil amendments in artificially contaminated soil. *Adv Environ Health Res* 2014; 2(4): 251-62.
18. Yang J, Sun H. Degradation of γ -hexachlorocyclohexane using carboxymethylcellulose-stabilized Fe/Ni nanoparticles. *Water Air Soil Pollut* 2015; 226: 280-95.
19. He F, Zhao D, Liu J, Roberts CB. Stabilization of Fe-Pd nanoparticles with sodium carboxymethyl cellulose for enhanced transport and

- dechlorination of trichloroethylene in soil and groundwater. *Ind Eng Chem Res* 2007; 46(1): 29-34.
20. He F, Zhao D. Preparation and characterization of a new class of starch-stabilized bimetallic nanoparticles for degradation of chlorinated hydrocarbons in water. *Environ Sci Technol* 2005; 39(9): 3314-20.
 21. Xiong Z, Zhao D, Pan G. Rapid and complete destruction of perchlorate in water and ion-exchange brine using stabilized zero-valent iron nanoparticles. *Water Res* 2007; 41(15): 3497-505.
 22. Wang Q, Snyder S, Kim J, Choi H. Aqueous ethanol modified nanoscale zerovalent iron in bromate reduction: synthesis, characterization, and reactivity. *Environ Sci Technol* 43(9): 3292-9.
 23. Wang W, Jin Z, Li T, Zhang H, Gao S. Preparation of spherical iron nanoclusters in ethanol-water solution for nitrate removal. *Chemosphere* 65(8): 1396-404.
 24. Choi H, Al-Abed SR, Agarwal S, Dionysiou DD. Synthesis of reactive nano-Fe/Pd bimetallic system-impregnated activated carbon for the simultaneous adsorption and dechlorination of PCBs. *Chem Mater* 2008; 20(11): 3649-55.
 25. Zhu H, Jia Y, Wu X, Wang H. Removal of arsenic from water by supported nano zero-valent iron on activated carbon. *J Hazard Mater* 2009; 172(2-3): 1591-6.
 26. Nabar G, Ramachandran C. Quantitative determination of perchlorate ion in solution. *Anal Chem* 1959; 31(2): 263-5.
 27. Fortune WB, Mellon M. Determination of iron with O-phenanthroline: a spectrophotometric study. *Ind Eng Chem Anal Ed* 1938; 10(2): 60-64.
 28. Bezerra MA, Santelli RE, Oliveira EP, Villar LS, Escalera LA. Response surface methodology (RSM) as a tool for optimization in analytical chemistry. *Talanta* 2008; 76(5):965-77.
 29. Boyacı IH. A new approach for determination of enzyme kinetic constants using response surface methodology. *Biochem Eng J* 2005; 25(1): 55-62.
 30. Montgomery SL. Permian bone spring formation: sandstone play in the Delaware basin, Part II-Basin. *AAPG bulletin* 1997; 81(9): 1423-34.
 31. Gu B, Dong W, Brown GM, Cole DR. Complete degradation of perchlorate in ferric chloride and hydrochloric acid under controlled temperature and pressure. *Environ Sci Technol* 2003;37(10):2291-5.
 32. Chen JL, Al-Abed SR, Ryan JA, Li Z. Effects of pH on dechlorination of trichloroethylene by zero-valent iron. *J Hazard Mater* 2001; 83(3):243-54.
 33. Gao H, Liu M, Liu J, Dai H, Zhou X, Liu X, *et al.* Medium optimization for the production of avermectin B1a by *Streptomyces avermitilis* 14-12A using response surface methodology. *Bioresour Technol* 2009; 100(17): 4012-16.
 34. Su JJ, Zhou Q, Zhang HY, Li YQ, Huang XQ, Xu YQ. Medium optimization for phenazine-1-carboxylic acid production by a *gacA qscR* double mutant of *Pseudomonas* sp. M18 using response surface methodology. *Bioresour Technol* 2010; 101(11): 4089-95.